

# Characterization Of Structures Of Equivalent Tissue With a Pixel Detector

M.C GRADOS LUYANDO\*, B. DE CELIS ALONSO, E. MORENO BARBOSA, M.I. MARTÍNEZ HERNÁNDEZ, J.M. HERNÁNDEZ LÓPEZ AND G. TEJEDA MUÑOZ

<sup>1</sup>Benemérita Universidad Autónoma de Puebla

\*Email: [carminagl87@gmail.com](mailto:carminagl87@gmail.com)

Published online: August 07, 2017

The Author(s) 2017. This article is published with open access at [www.chitkara.edu.in/publications](http://www.chitkara.edu.in/publications)

**Abstract** Research using hybrid pixel detectors in medical physics is on the rise. Timepix detectors have arrays of  $256 \times 256$  pixels with a resolution of  $55 \mu\text{m}$ . Here, and by using Timepix counts instead of Hounsfield units, we present a calibration curve of a Timepix detector analog to those used for CT calibration. Experimentation consisted of the characterization of electron density in 10 different kinds of tissue equivalent samples from a CIRS 062M phantom (lung, 3 kinds of bones, fat, breast, muscle, water and air). Radiation of the detector was performed using an orthodontic X-ray machine at 70 KeV and .06 second of tube current with a purpose-built aluminum collimator. Data acquisition was performed at 1 frame per second and taking 3 frames per phantom. We were able to find a curve whose behavior was similar to others already published. This will lead to the verification of the usage of Timepix for identification of different tissues in an organ.

**Keywords:** Timepix, Computed Tomography, Dose

## 1. INTRODUCTION

Hybrid pixel detectors are getting started to be used in medical research in the last few years [1] [2], they have important advantages to be use in the field. Timepix is a hybrid pixel detector developed by CERN collaboration for particle detections [3].

It has a good sensitivity [4] and good resolution for medical imaging, having this in mind we have decided to find a calibration curve analog to the one used for CT calibration. The idea is to find the correspondence Timepix counts to each value of tissue in Hounsfield Units already known. Hounsfield

Journal of Nuclear  
Physics, Material  
Sciences, Radiation and  
Applications  
Vol-5 No-1  
August 2017  
pp. 79–89

---

Grados Luyando, M.C.  
de Celis Alonso, B.  
Moreno Barbosa, E.  
Martínez Hernández,  
M.I.  
Hernández López, J.M.  
Tejeda Muñoz, G.

---

Units go from -1000 to 1000 depending of the level of brightness in the x-ray plaque, where -1000 is air or less density, and 1000 correspond to bone of higher density, passing through 0 which is water. Using the detector in ToT mode, we have radiated the samples using the minimum tube current 0.06 sec, 3 times each one, having 3 different matrixes of 65,536 numbers. Once the data has been collected, an algorithm in C++ give us a characteristic number for each sample, this number give the counts number analog to the CT number in HU. We where able to find a curve with the same behavior as in CT [5], with the advantage of less time of exposure and therefore less dose.

## 2. MATERIALS AND METHODS

### 2.1 The Detector

Timepix device is a hybrid detector with an arrangement of  $256 \times 256$  pixels with a resolution of  $55 \mu\text{m}$ , its dimensions are  $14.08 \text{ mm} \times 14.08 \text{ mm}$ . Made by 2 main parts, the detection, which is an ionization chamber, bump-bonded to a CMOS electronic layer, part 2, Fig. 1, each matrix pixel is connected to his respective preamplifier, discriminator and digital counter integrated on the read out chip. Timepix operates in 3 different modes: 1) Single particle counting, 2) Time over Threshold and 3) Arrival time mode [3].

Single particle counting: It counts an event for each particle over threshold, Time over Threshold: this mode counts the time or clocks while the energy remains above the threshold, giving a number proportional to that

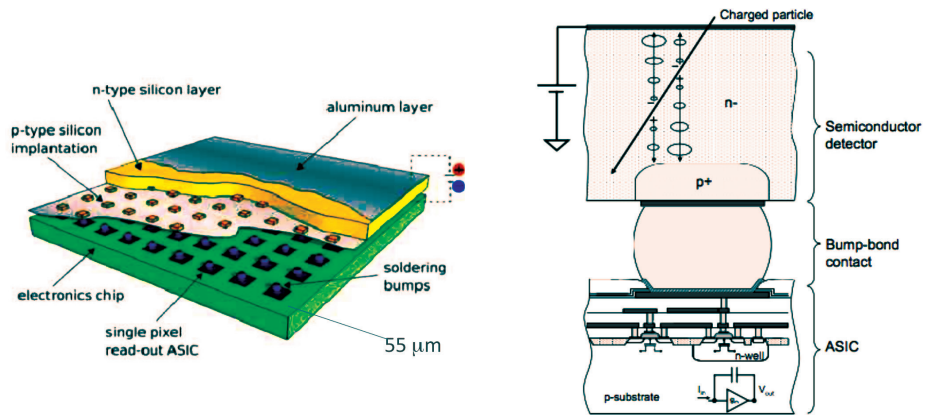


**Figure 1:** a) View of a sensor bump-bonded to a read our chip. Adapted [10], and b) detection diagram [11]

---

energy, Arrival mode: Counts the time between the trigger and an event over the threshold.

In other works, the performance of this detector has been studied for X-rays [6] [7], heavy charged particles [8], ultra cold neutrons [9], cosmic radiation and with electron optics.

Characterization  
of structures of  
equivalent tissue  
with a pixel  
detector

## 2.2 Imaging System

An orthodontic x-ray source GNATUS with 70 KeV, 7 mA and .06 sec of tube current, with a Tungsten target tube and a  $.8 \times .8$  mm emission spot [12], after a purpose-built aluminum collimator made of 2 plaques of 3 mm each Fig. 2 for 99% attenuation of the beam, and an aperture of  $3 \times 3$  cm. The distance from the detector to the tube is 5 cm. Between these, the equivalent tissue samples CIRS, electron density phantom model 062M [13] (lung inhale, lung exhale, 3 bones, fat, breast, muscle, water and air) are placed for being radiated.

## 2.3 Data Acquisition

The device is connected to the interface FITPix, which has a serial readout speed around 100 frames per second in single layer [14]. Images have been obtained with software PixetPro. Each sample has been radiated 3 times at the lowest current tube 0.06 sec; To T mode, 1 frame per second and with threshold at 10. To T mode allows the detector to measure directly the energy

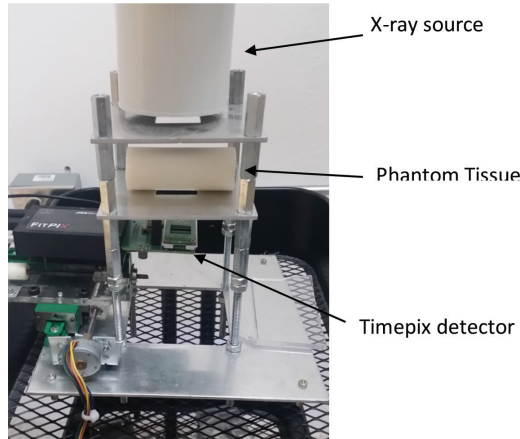


**Figure 2:** Picture of the imaging system, the x-ray source, the collimator and the detector.

Grados Luyando, M.C.  
de Celis Alonso, B.  
Moreno Barbosa, E.  
Martínez Hernández,  
M.I.  
Hernández López, J.M.  
Tejeda Muñoz, G.

in each pixel, using a defined threshold, the amount of energy deposite in the pixel works as a capacitor and the time of discharge until it get to the threshold defined is the count of that pixel. Bias voltage used for this experiment was 100 V. The three shots are consecutive and the data acquired has been saved separately in different files.

## 2.4 Data Analysis

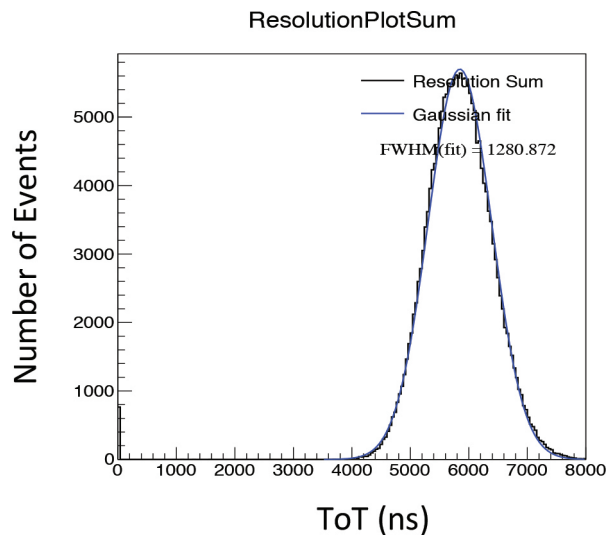
A C++ algorithm has been write for the data analysis, the algorithm makes an average from the 3 matrixes data, make a fit and measure FWHM. Each FWHM is characteristic from the material, this value is saved and used to make a graphic vs mass density and relative electronic density with software Origin Pro 8. For our purposes the energy absorbed by the detector is not of our consideration, nevertheless the proper energy calculations can be found at [15].

## 3. RESULTS

The first part of the results are the single curves founded of each phantom tissue, Fig. 2 – Fig. 11, with the proper fit and calculation of them FWHM, the axis graphics are ToT Vs Number of events, followed by the graphic of all together being normalized to the maximum value. Table 1 show the correspondence values founded for each phantom tissue, and finally the analog to CT with the same behavior.

**Table 1:** Correspondence between mass density, RED and counts founded in the characterization.

Tissue	Mass density (g/cc)	Relative Electronic Density	FWHM (ua)
Air	0	0	1341
Lung Inhale	0.2	0.19	1280
Lung Exhale	0.5	0.489	1126
Adipose	0.96	0.949	1084
Breast	0.99	0.976	953
Muscle	1.06	1.043	915
Water	1	1	842
Bone3	1.16	1.117	644



Characterization  
of structures of  
equivalent tissue  
with a pixel  
detector

---

**Figure 3:** Characteristic curve of lung inhale.

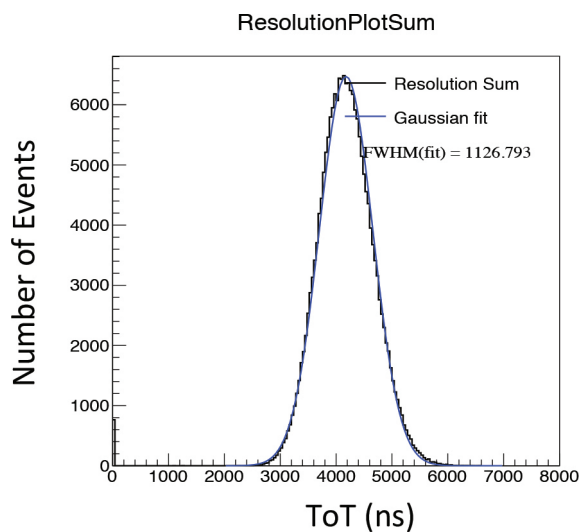


**Figure 4:** Analog curves to CT with mass density and relative electronic density (RED).

---

Grados Luyando, M.C.  
de Celis Alonso, B.  
Moreno Barbosa, E.  
Martínez Hernández,  
M.I.  
Hernández López, J.M.  
Tejeda Muñoz, G.

---

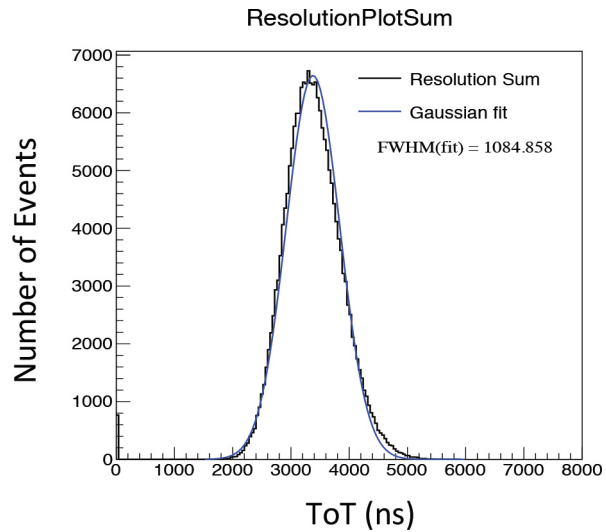


**Figure 5:** Characteristic curve of adipose.

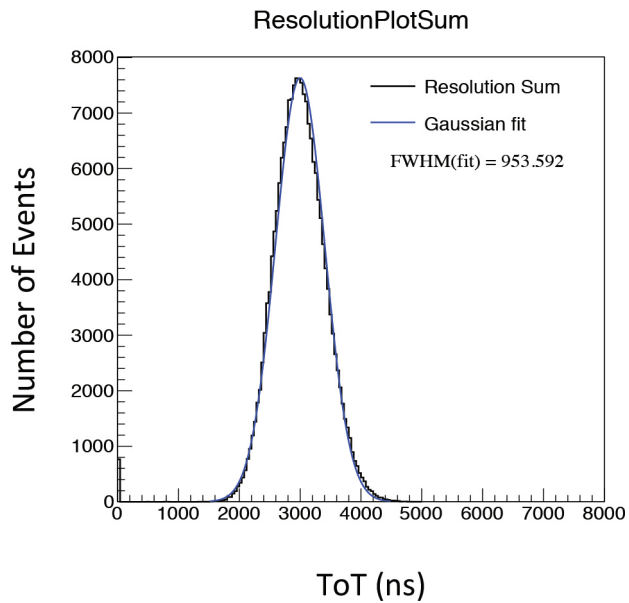
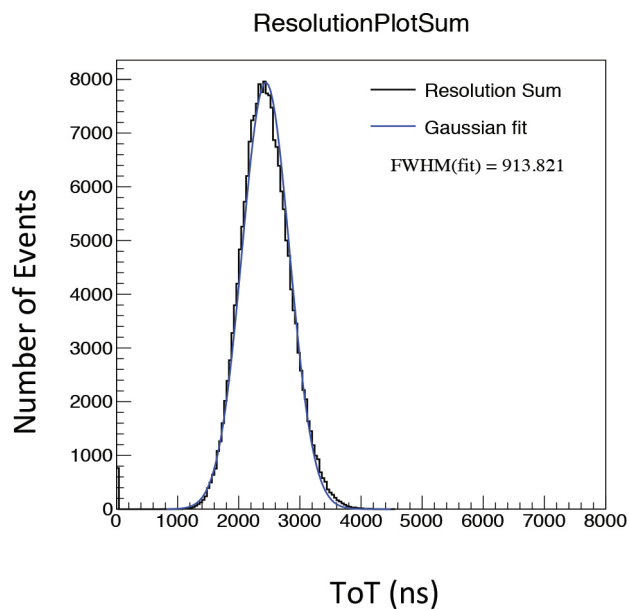


**Figure 6:** Characteristic curve of breast.



Characterization  
of structures of  
equivalent tissue  
with a pixel  
detector

---

**Figure 7:** Characteristic curve of muscle.

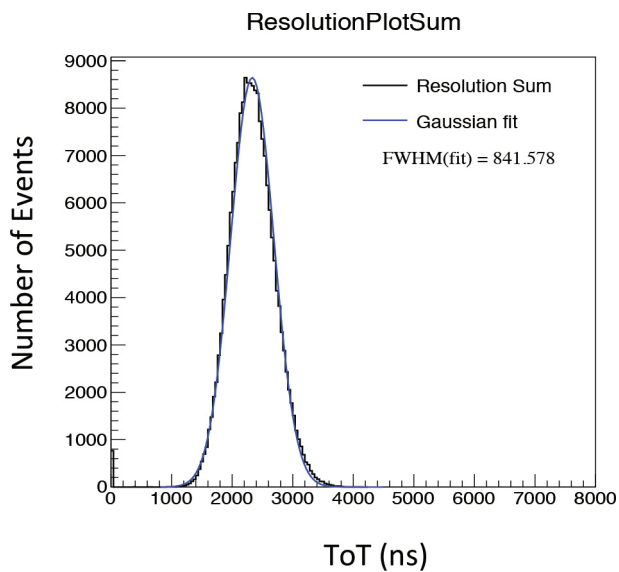


**Figure 8:** Characteristic curve of water.

---

Grados Luyando, M.C.  
de Celis Alonso, B.  
Moreno Barbosa, E.  
Martínez Hernández,  
M.I.  
Hernández López, J.M.  
Tejeda Muñoz, G.

---

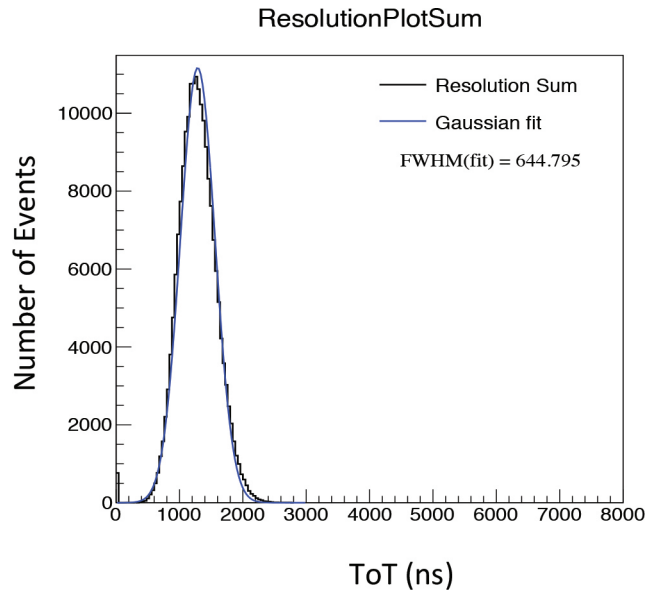


**Figure 9:** Characteristic curve of bone 1.

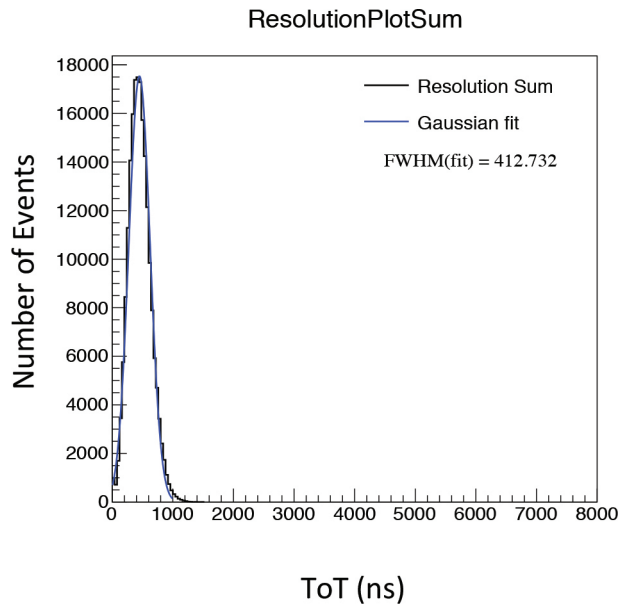
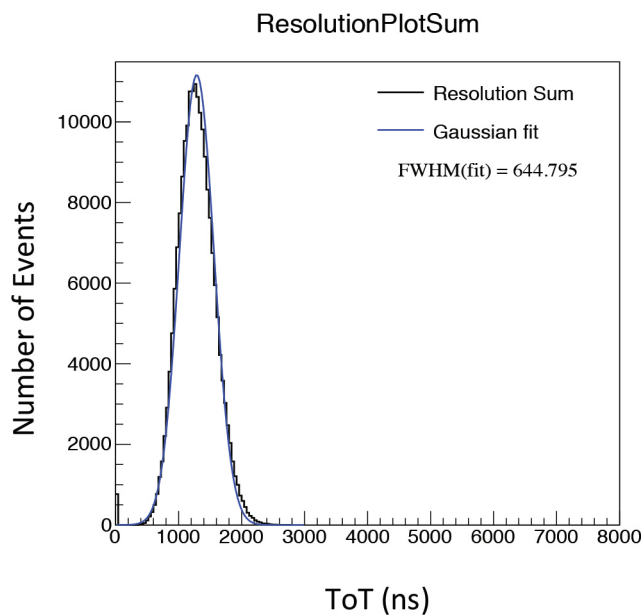


**Figure 10:** Characteristic curve of bone 2.



Characterization  
of structures of  
equivalent tissue  
with a pixel  
detector

**Figure 11:** Characteristic curve of bone 3.

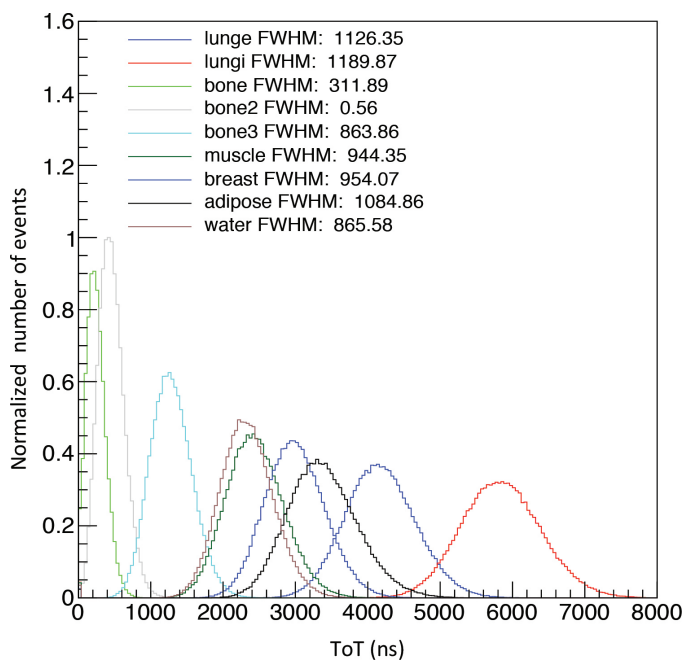


**Figure 12:** Characteristic curves of all tissues together and normalized to the max. value.

Grados Luyando, M.C.  
de Celis Alonso, B.  
Moreno Barbosa, E.  
Martínez Hernández,  
M.I.  
Hernández López, J.M.  
Tejeda Muñoz, G.

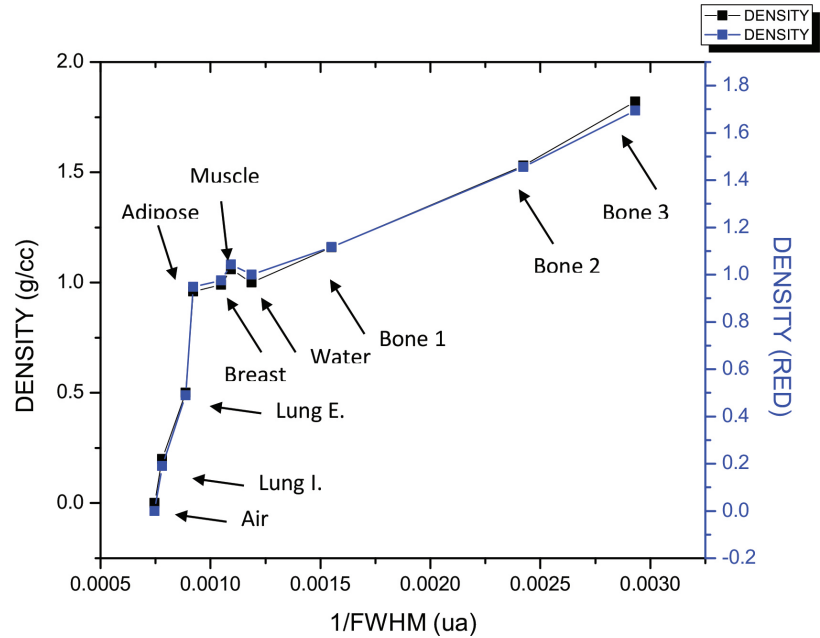


**Figure 4:** Analog curves to CT with mass density and relative electronic density (RED).

Bone2	1.53	1.456	412
Bone1	1.82	1.695	341

## CONCLUSIONS

We founded a relation between counts and HU, the analog graph behaves as the one already known for CT [5], with this result we were able to find the correspondence of Timepix counts to each tissue. This will lead to the verification of the usage of Timepix for identification of different tissues in an organ. And the possibility to calculate treatment planning using the data of the pixel detector improving the resolution of the images.

## REFERENCE

- [1] Franca Cassol Brunner: First K-Edge Imaging With a Micro-CT Based on the XPAD3 Hybrid Pixel Detector. IEEE Transactions on Nuclear Science 60(1), 103–108 (February 2013)

- 
- [2] P. Delpierre, (February 2007) e.: PIXSCAN, Pixel detector CT-scanner for small animal imaging. Nuclear Instruments and Methods in Physics Research Section A: Accelerators, Spectrometers, Detectors and Associated Equipment(1-2), 425–428.
- [3] CERN: Medipix. Available at: <https://medipix.web.cern.ch/medipix/pages/medipix2/timepix.php>
- [4] M. Esposito, e.: Energy sensitive Timepix silicon detector for electron imaging. Nuclear Instruments and Methods in Physics Research A (October 2011)
- [5] J. Seco, (February 2006) P.: Assessing the effect of electron density in photon dose calculations. MEDICAL PHYSICS 33(2).
- [6] J. Jakubek: (August 2009) Energy-sensitive X-ray radiography and charge sharing effect in pixelated detector. Nuclear Instruments and Methods in Physics Research 607(1).
- [7] Zemlicka: Energy and position sensitive Pixel detector Timepix for X-ray fluorescence imaging. Nuclear Instruments and Methods in Physics Research 607(202) (2009)
- [8] J. Jakubek: Pixel detectors for imaging with heavy charged particles. Nuclear Instruments and Methods in Physics Research 591(1) (2008)
- [9] J. Jakubek: A coated pixel device TimePix with micron spatial resolution for UCN detection. Nuclear Instruments and Methods in Physics Research 600 (2009)
- [10] Boog, R.: Energy calibration procedure of a pixel detector. (2013)
- [11] Campbell, M.: Charged particle detection using the timepix and timepix3 chips and future plans. (Accessed 2012) Available at: [https://www2.physics.ox.ac.uk/sites/default/files/2012-03-27/mcampbell\\_oxford\\_pdf\\_14057.pdf](https://www2.physics.ox.ac.uk/sites/default/files/2012-03-27/mcampbell_oxford_pdf_14057.pdf)
- [12] GNATUS Available at: [http://www.gnatus.com.br/site/esp/produtos\\_show.php?id=1133&cat=813&scat=imagen](http://www.gnatus.com.br/site/esp/produtos_show.php?id=1133&cat=813&scat=imagen)
- [13] CIRS Available at: <http://www.cirsinc.com/products/all/24/electron-density-phantom/>
- [14] Advacam In: Advacam. Available at: <http://www.advacam.com/en/products/fitpixkit>
- [15] A. Butler, P.: Measurement of the energy resolution and calibration of hybrid pixel detectors with GaAs:Cr sensor and Timepix readout chip. Physics of Particles and Nuclei Letters 12(1) (January 2015)
- 

Characterization  
of structures of  
equivalent tissue  
with a pixel  
detector